ELSEVIER

Journal of Chromatography A, 791 (1997) 255–267

JOURNAL OF CHROMATOGRAPHY A

On-line concentration of neutral analytes for micellar electrokinetic chromatography
II. Reversed electrode polarity stacking mode

Joselito P. Quirino*, Shigeru Terabe

Faculty of Science, Himeji Institute of Technology, Kamigori, Hyogo 678-12 Japan

Received 15 April 1997; received in revised form 10 July 1997; accepted 16 July 1997

Abstract

Basic conditions for the on-line neutral sample concentration by reversed electrode polarity stacking mode for micellar electrokinetic chromatography are developed theoretically and experimentally verified. Stacking is mainly dependent on analyte retention factors and nature of the pseudostationary phases. More than an order of magnitude improvement in concentration detection limit is achieved for resorcinol using high molecular mass surfactants. © 1997 Elsevier Science B.V.

Keywords: Sample stacking; Sample handling; Injection methods

1. Introduction

Since its emergence in 1984 [1], micellar electrokinetic chromatography (MEKC) has been acknowledged as a very powerful separation tool for electrically neutral solutes. The separation mechanism is an interesting cross between chromatography and electrophoresis. Concentration sensitivity is rather poor as the other CE techniques because only small volumes of sample solution can be injected. Applicability is often limited to samples like pharmaceuticals where the concentration of the analytes of interest can easily be adjusted to yield reasonable detector responses. To expand its use for the analysis of real samples, the need to develop compatible focusing techniques is very urgent.

Only a few papers have appeared pertaining to the on-line sample enrichment of neutral analytes by sample stacking for MEKC [2–4], and improvements in sensitivity are often not akin with those obtainable in CZE for charged analytes [5–11]. One of the improvements for MEKC is reversed electrode polarity stacking mode (REPSM) first reported by Liu et al. using sodium dodecyl sulfate (SDS) at a concentration slightly above the critical micelle concentration (cmc) in the sample matrix [2]; a maximum sensitivity enhancement value of 85 based on peak area was noted. Briefly, in REPSM samples are prepared in low conductivity matrices and are injected as long plugs into the capillary. Effective electrophoretic velocities in the sample zone are much greater than that in the separation zone because of the enhanced field in the sample zone. Samples will therefore stack as concentrated zones in the concentration boundary between the sample and separation zones. Polarity of the voltage applied is

*Corresponding author.

0021-9673/97/$17.00
PII S0021-9673(97)00796-6

initially negative to facilitate stacking of the analytes and removal of the sample matrix. Once the current reached 97–99% of the predetermined current at this configuration, the polarity is switched to positive to enable the separation and detection of stacked zones.

In this paper, we describe the theory and practise of REPSM. Stacking is evaluated based on analyte retention factors and the nature of the pseudo-stationary phases. Non-micellar solutions of low conductivity are used as sample matrix. Micelles are then electrokinetically introduced to the sample solution at negative polarity. Manipulation of retention factors by increasing the concentration of surfactant or addition of non-ionic surfactant improved sensitivity enhancements. Significant detector response improvements are confirmed experimentally.

2. Theory

2.1. General remarks on reversed electrode polarity stacking mode micellar electrokinetic chromatography (REPSM MEKC)

When we speak of REPSM MEKC (Fig. 1), we consider not only the stacking step but rather all the procedures embraced therein from sample preparation to detection of analyte zones. Three steps are involved: (1) (Fig. 1A), long hydrodynamic injection of the sample solution prepared in a low conductivity matrix (S) after filling the capillary with high conductivity micellar solution (BGS) only: (2) (Fig. 1B), application of voltage at negative polarity where the inlet and outlet vials contain the BGS: and (3) (Fig. 1C and D), switching polarity from negative to

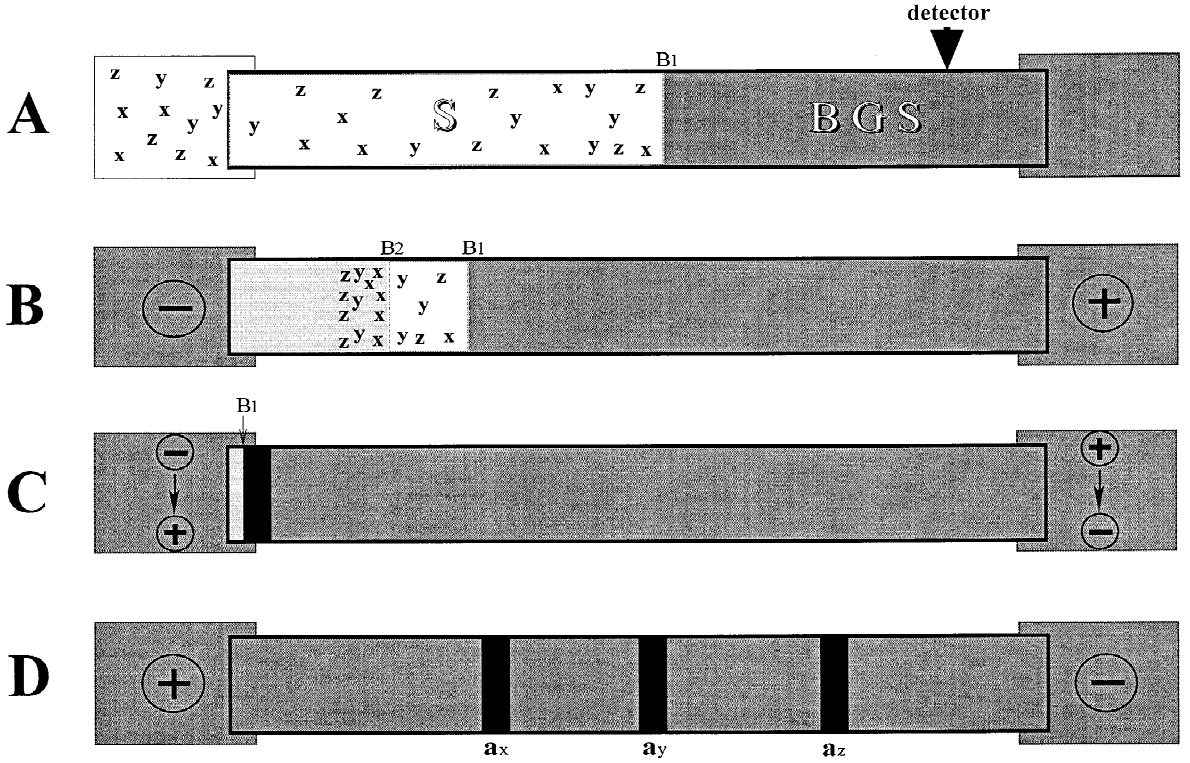

Fig. 1. Behavior of micelles and neutral analytes during REPSM MEKC. (A) Starting situation; (B) micelles enter the capillary and carry with it neutral analytes a, $k(a_x)>k(a_y)>k(a_z)$; (C) micelles and neutral analytes stack at the concentration boundary (B_1) and polarity is switched later to positive; (D) separation and later detection of zones.

positive when the current reached 97–99% of the predetermined current at negative polarity, maintaining the voltage until all peaks of interest are detected. REPSM therefore entails several complicated phenomena.

In step 1, samples are prepared in non-micellar low conductivity matrices or simply water such that the electrophoretic velocity of micelles that will enter the S region will be greater than those in the BGS region. S region (Fig. 1A) is the unshaded area with neutral analytes a (a_x, a_y, a_z) and BGS region is the heavily shaded area. In step 2, voltage is applied at negative polarity to electrokinetically inject the micelles (Fig. 1B, lightly shaded part of S region) from the cathodic vial that will carry the neutral analytes toward the anode. High retention factor (k) compounds travel faster than low k compounds. Buffer anions also enter the S region. At the same time, the sample matrix is being pumped out from the capillary to the cathodic vial by the electroosmotic flow and is being replaced by the BGS coming from the anodic vial. Removal of the sample matrix lessens the dispersive effects caused by laminar flow brought by the mismatch of local electroosmotic velocities of the low and high conductivity regions [10]. Step 3 is performed when most neutral analytes in S (Fig. 1C) has been considerably focused upon passage through the concentration boundary (B_1), that is when the measured currents are between 97 and 99% of the predetermined current. The separation and later detection of stacked zones are finally shown in Fig. 1D.

2.2. Initial behavior of micelles

With the arrangement in Fig. 1B, the migration velocity of anionic micelles in the S region, v_{mc}(S), or BGS region, v_{mc}(BGS), independently is the sum of two vector quantities, the averaged bulk velocity of the electroosmotic flow, v_{eof}(ave) and the electrophoretic velocity of the micelle in the S region, v_{ep}(mc,S), or BGS region, v_{ep}(mc,BGS), respectively (Eqs. (1) and (2)) [3].

$$v_{mc}(S) = v_{eof}(ave) + v_{ep}(mc,S) \quad (1)$$

$$v_{mc}(BGS) = v_{eof}(ave) + v_{ep}(mc,BGS) \quad (2)$$

The v_{eof}(ave) is given by Eq. (3) [5].

$$v_{eof}(ave) = \frac{\gamma x v_{eof}(S) + (1-x) v_{eof}(BGS)}{\gamma x + (1-x)} \quad (3)$$

where v_{eof}(S) and v_{eof}(BGS) are the electroosmotic flow velocities of S and BGS respectively, measured in their homogenous systems. The enhancement factor (γ) is equal to the resistivity ratio of S and BGS and x is the fraction of the capillary filled with S. The value of v_{eof}(ave) changes from v_{eof}(S) to v_{eof}(BGS) as x approaches 0. The electrophoretic velocities of the micelles in the two regions are given by Eqs. (4) and (5),

$$v_{ep}(mc,S) = \mu_{ep}(mc) E_S \quad (4)$$

$$v_{ep}(mc,BGS) = \mu_{ep}(mc) E_{BGS} \quad (5)$$

where μ_{ep}(mc) is the electrophoretic mobility of the micelle. The field strength in the S region (E_S) and BGS region (E_{BGS}) are given by Eqs. (6) and (7), respectively [5],

$$E_s = \gamma E_0 / [\gamma x + (1-x)] \quad (6)$$

$$E_{BGS} = E_0 / [\gamma x + (1-x)] \quad (7)$$

where E_0 is equal to V/L (voltage V applied across a capillary with length L). Both the field strengths in the S and BGS regions increase with the decrease in x based on Eqs. (6) and (7), but to a greater extent in the S region with a factor equal to γ. A corresponding increase in v_{ep}(mc,S) and v_{ep}(mc,BGS) will then follow. A very high value for γ is then desired such that the field will be greatly distributed to the S zone alone. Essentially, v_{ep}(mc,S), v_{ep}(mc,BGS) and v_{eof}(ave) change with the alleviation of x, but the change in v_{eof}(ave) and v_{ep}(mc,BGS) is not large compared to the change in v_{ep}(mc,S).

Let us consider v_{eof}(ave) as equal to v_{eof}(S) [10]. A certain fraction of the capillary filled with S which we denote as the ultimate maximum fill fraction x_{max} (Eq. (8)) will only permit the migration of micelles into the capillary [10].

$$x_{max} = \frac{\mu_{ep}(mc)}{\mu_{eof}(S)} \quad (8)$$

where $\mu_{eof}(S)$ is the electroosmotic mobility or the coefficient of electroosmotic flow of S. Note that the micelles will not enter into the S region from the BGS zone on the anodic side. Fig. 2 depicts the theoretical plots of $v_{mc}(S)$, $v_{eof}(S)$ and $v_{ep}(mc,S)$ generated by a set of parameters. For these plots, we used the values obtained in the system in Table 3. The value of γ was calculated based on the conductivity of BGS (5.980 mS/cm) and S (0.875 mS/cm) and $v_{eof}(S)$ was calculated based on the migration time of a neutral marker (mesityl oxide) in S represented by the 5 m*M* sodium dihydrogen phosphate–10 m*M* sodium tetraborate buffer (pH 7). The curve of $v_{mc}(S)$ intersecting the *x*-axis yielded x_{max} and had a value of 0.64 based on Eq. (8). For values of *x* lower than the x_{max} (left side of the intersection), $v_{mc}(S)$ from Eq. (1) is negative or towards the anode since $v_{ep}(mc,S)$ is greater in magnitude than $v_{eof}(ave)$. Micelles from the cathodic vial therefore enter the capillary as previously shown in Fig. 1B. At this stage because of low field strength in the BGS zone, $v_{mc}(BGS)$ from Eq. (2) is positive or towards the cathode since $v_{eof}(ave)$ is much greater in magnitude than $v_{ep}(mc,BGS)$. Micelles in the injected BGS region therefore migrate toward the cathode (heavily shaded area in Fig. 1A moves to the left as shown in Fig. 1B). Also, buffer electrolytes in the injected BGS depending on their charge migrate towards the anode or the cathode.

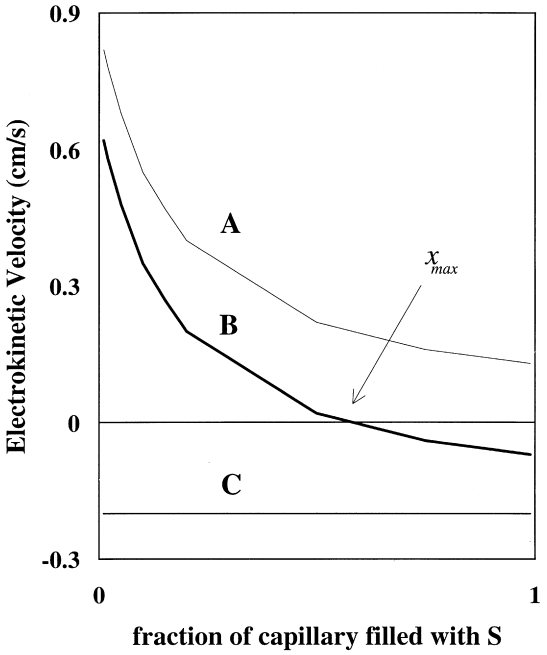

Fig. 2. Theoretical plots of the electrokinetic velocities against the fraction of capillary filled with sample solution under negative polarity. (A) Electrophoretic velocity of the micelle in the sample region $v_{ep}(mc,S)$; (B) migration velocity of the micelle in the sample region $v_{mc}(S)$; (C) electroosmotic flow velocity of the sample solution $v_{eof}(S)$; γ, 6.83; (E) −310.08 V/cm; $\mu_{eof}(S)$, $6.45 \cdot 10^{-4}$ cm^2/Vs; $\mu_{ep}(mc)$, $-4.12 \cdot 10^{-4}$ cm^2/Vs.

The concept of x^*_{max} (Eq. (9)) is then proposed, which is the maximum fraction of the capillary filled with S that will permit movement of neutral analytes to the concentration boundary.

$$x^*_{max} = x_{max}\frac{k_S}{k_S + 1} \quad (9)$$

The value of x^*_{max} increases with the increase in the retention factor in the S region (k_S) from Eq. (9). Take a capillary simply filled with S as an example, upon application of voltage at negative polarity, some volume of S corresponding to some amount of each analyte previously found in the capillary will just be lost to the cathodic vial until each corresponding x^*_{max} is reached. Therefore, based on Eq. (9) and when the fraction of the capillary injected with S exceeds the x^*_{max} of all test analytes, a higher fraction of the analytes with high k_S will be stacked compared to analytes with low k_S.

2.3. Behavior of neutral analytes in the stacking boundary

Assuming that the flux of ions out of the concentration boundary (B_1) is equal to the flux toward it, B_1 is therefore pseudostationary and moves with a velocity equal to $v_{eof}(ave)$ [12]. When B_2 crosses B_1 in Fig. 1B, micelles and neutral analytes solubilized in it stack in B_1 since the experienced field drops abruptly. The electrophoretic velocity of micelles shifts from $v_{ep}(mc,S)$ to $v_{ep}(mc,BGS)$. The migration velocity difference between the stacked micelle and B_1 is equal to $v_{ep}(mc,BGS)$ [3]. This small difference in migration velocities will cause the stacked micelles to leave B_1 prior to the total removal of the

sample matrix. The same follows for neutral analytes solubilized in the stacked micelles. The migration velocity of a in the S region, v_a(S) and BGS region, v_a(BGS), is given by Eqs. (10) and (11), respectively.

$$v_a(S) = v_{eof}(ave) + v^*_{ep}(a,S) \text{ where } v^*_{ep}(a,S) = v_{ep}(mc,S)\frac{k_S}{k_S + 1} \quad (10)$$

$$v_a(BGS) = v_{eof}(ave) + v^*_{ep}(a,BGS) \text{ where } v^*_{ep}(a,BGS) = v_{ep}(mc,BGS)\frac{k_{BGS}}{k_{BGS} + 1} \quad (11)$$

where v^*_{ep}(a,S) and v^*_{ep}(a,BGS) are the effective electrophoretic velocities of a in the S and BGS regions respectively and k_{BGS} is the retention factor in the BGS zone. The value of v^*_{ep}(a,BGS) is then the migration velocity difference between the stacked neutral analyte and B_1 that will cause the stacked neutral analyte to leave B_1.

2.4. Improving stacking via manipulation of retention factors

Stacking enhancement factor given in terms of peak height, SE_{height}, (Eq. (12)) formerly coined as stacking efficiency in terms of peak height [3] is expressed as the ratio of the heights obtained with stacking, H_{stack}, versus the heights obtained with a normal MEKC injection, H, where the same sample solution is used. The value of H in this particular study is obtained from a 2-s hydrodynamic injection.

$$SE_{height} = \frac{H_{stack}}{H} \quad (12)$$

Since this ratio is not only dependent on how much the analyte stacked together when they cross the concentration boundary but also on other factors (i.e., laminar flow produced by the mismatch of local electroosmotic velocities which causes an additional dispersive effect [5]), we changed stacking efficiency to stacking enhancement factor. The percentage of sample effectively stacked into a peak from the total volume of sample injected (%SE) is then described by Eq. (13),

$$\%SE = \frac{SE_{height}}{SE_{height}(expected)}100\% \quad (13)$$

where SE_{height}(expected) is the expected stacking enhancement factor based on peak height (e.g. for a 240-s injection REPSM compared to a 2-s hydrodynamic injection the value is 120). We therefore assumed here that with stacking, the peak height is directly proportional to the injection time. Another relation is recovery (%R) (Eq. (14)) which depicts the amount of analytes that were able to resist the electroosmotic flow during step 2 [3].

$$\%R = \frac{SE_{area}}{SE_{area}(expected)}100\% \quad (14)$$

SE_{area} is the ratio of corrected peak area obtained from stacking and corrected peak area obtained from a normal MEKC injection and SE_{area}(expected) is the expected stacking enhancement factor in terms of peak area, which is numerically equivalent to SE_{height}(expected). Stacking efficiencies in terms of area [3] is also changed in this paper to stacking enhancement factors for consistency. Note that whereas %SE depicts the amount of analytes effectively stacked into a peak, %R depicts the amount of analytes that were able to resist the electroosmotic flow. The ratio of %SE and %R (%Stacked) will then describe the amount of analyte that is effectively stacked into a peak from the total amount of analyte that resisted the electroosmotic flow during step 2 (Eq. (15)).

$$\%Stacked = \frac{\%SE}{\%R}100\% \text{ or } \frac{SE_{height}}{SE_{area}}100\% \quad (15)$$

A value of 100% would mean that all the analytes that are brought to the concentration boundary are stacked effectively. This value describes to some extent how much the analyte stacked together when they reached the concentration boundary if they were able to resist the electroosmotic flow and it shows the direct relation between SE_{height} and SE_{area}. In addition, whereas %Stacked is ideally a constant given a set of analytical parameters, independent of k but dependent on the γ and the nature of the pseudostationary phase, SE_{height} and SE_{area} are not

constants and are dependent on k, γ and the nature of the pseudostationary phase.

In normal MEKC separations, k increases with the increase in the concentration of surfactant. In this case, we deal with a region (S region) that is gradually filled with anionic micelles from the cathodic vial in step 2 through electrokinetic introduction. Provided γ is constant, we assume that the concentration of the micelle in the S region is directly proportional and lower than the concentration of the micelle in the BGS region. Therefore, an increase in the concentration of micelle in the BGS will cause an increase in the concentration of micelle in the S region during step 2, which in turn increases k_S, which in turn increases x^*_{max} (Eq. (9)). As noted earlier for x^*_{max}, a consequence of the increase of which is an increase in the amount of analytes available for stacking or an increase in SE_{area}. Ultimately, assuming that %Stacked will not change considerably with the increase in the concentration of surfactant, the increase in the concentration of micelle in the BGS may therefore increase SE_{height}. In this study we are more interested in SE_{height} primarily because it is directly related to the hoped improvements for detection limits. Increasing the value of k_S by addition of a non-ionic surfactant to form a mixed micelle [13] is another approach to improve SE_{height}.

3. Experimental

3.1. Apparatus

Capillary electrophoresis and reversed electrode polarity stacking mode (REPSM) were carried out on a Hewlett Packard 3D capillary electrophoresis system (Waldbronn, Germany) equipped with fused-silica capillaries of 50 μm I.D. obtained from Polymicro Technologies (Phoenix, AZ, USA). Capillaries were thermostated at 20°C. Detection was performed at 210, 214 and 226 nm. The capillaries were conditioned and washed after each run according to our previous method [3]. Conductivity of sample and separation solutions was measured using a Horiba ES-12 conductivity meter (Kyoto, Japan).

3.2. Samples and reagents

All solutions were prepared from water purified with a Milli-Q system (Millipore, Bedford, MA, USA) and were filtered prior to use through 0.45-μm filters (Toyo Roshi, Japan). All reagents were obtained in the purest grade available. Resorcinol, 1,6-dihydroxynaphthalene, 1-naphthol, 2-naphthol, sodium tetraborate, sodium dodecyl sulfate (SDS) and polyoxyethylene lauryl ether (Brij 35) were purchased from Nacalai Tesque (Kyoto, Japan). Sodium dihydrogen phosphate was acquired from Wako Pure Chemicals (Osaka, Japan). Mesityl oxide and Sudan IV were obtained from Tokyo Kasei (Tokyo, Japan). Sample stock solutions were prepared with concentrations depending on their solubility in water and were diluted properly with water, or diluted buffer or separation solution to give sufficient peak heights.

Buffers were prepared accordingly from 100 m*M* sodium dihydrogen phosphate, 100 m*M* sodium tetraborate and 100 m*M* sodium hydroxide stock solutions. Separation solutions were prepared by dissolving appropriate amounts of surfactant/s into pertinent separation buffers. Butyl acrylate–butyl methacrylate–methacrylic acid copolymers, sodium salt (BBMA) supplied by Dai-ichi Kogyo Seiyaku (Kyoto, Japan) was purified by dialysis and solidified by freeze-drying. Sodium 10-undecylenate (SUA) oligomer was synthesized by Mr. Koji Iida as described by Palmer et al. [14]. Retention factors were determined using Sudan IV as marker of the micelle and mesityl oxide as marker of electroosmotic flow.

3.3. Procedure for REPSM MEKC

Samples prepared in a low conductivity matrix were injected at very long intervals into the capillary previously filled with separation solution. Sample solutions were introduced at the far from detector end of the capillary at 50 mbar or simply flushed at high pressure in some instances. Voltage was applied at negative polarity (−20 kV) and the current was monitored attentively. When the current reached 97–99% of the predetermined current, polarity was switched to normal mode (20 kV) to allow separation and detection.

4. Results and discussions

4.1. Choosing the sample matrix

Similar to our previous study with normal stacking mode [3], micelles in the sample zone are not necessary for stacking. Fig. 3 shows better sharpening of zones when samples are prepared with water (C) rather than with a 1/10 dilution of BGS (B). In a separate experiment, the same sharpening effect (water as sample matrix) is observed when the samples are prepared in 10 m*M* sodium dihydrogen phosphate–10 m*M* sodium tetraborate (no SDS, pH 8). Water is then utilized to prepare the S in order to maximize γ. We also tried injection of small plugs of BGS after long injections of S but the results obtained are similar to when there were no injections of BGS. The optimized REPSM MEKC electropherogram of the test naphthols is given in Fig. 4. With the conditions in Fig. 4B, detector responses increased with the increase in injection time which ceased after 240 s (around 37% of the capillary). Considering the speed of the injection procedure, the capillary is filled with S by flushing at high pressure prior to the application of voltage at negative polarity.

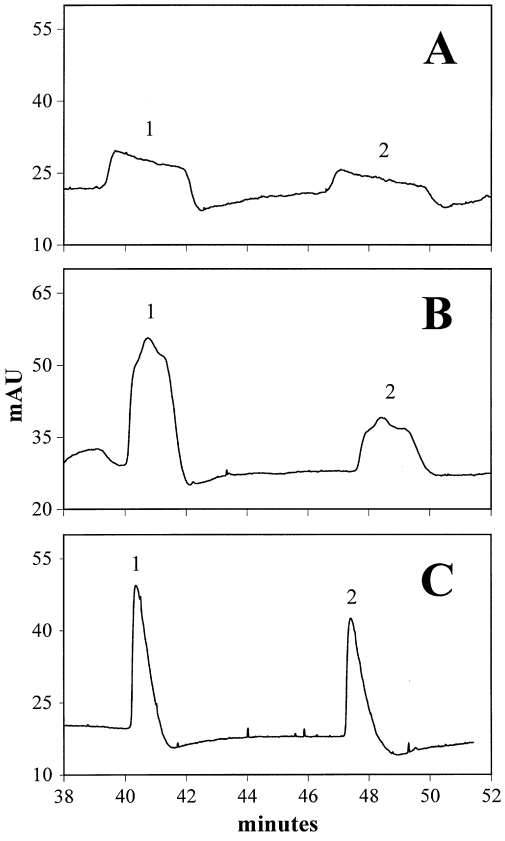

Fig. 3. Comparison of peak heights and shapes among different sample matrices. S, naphthols in BGS (A) one-tenth dilution of BGS (B), water (C); injection, 60 s without matrix removal (A), with matrix removal (B,C); BGS, 1% BBMA in 100 m*M* sodium dihydrogen phosphate–100 m*M* sodium tetraborate (pH 8); peaks: 1 (2-naphthol), 2 (1-naphthol); capillary, 63.5 cm (55 cm to detector); detection, 214 nm; see Section 3 for the other conditions.

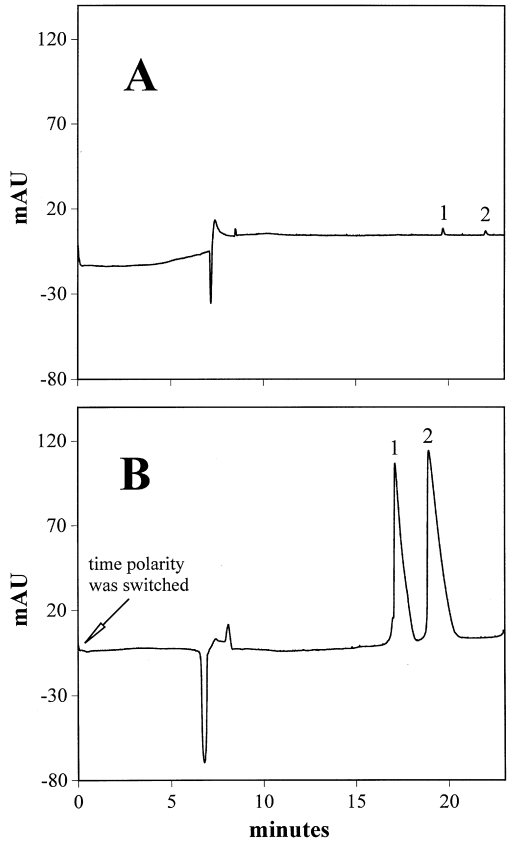

Fig. 4. Optimized REPSM electropherogram of naphthols with BBMA. Injection, 2 s (A), whole capillary filling with matrix removal (B); S, naphthols in water; BGS, 1% BBMA in 50 m*M* sodium dihydrogen phosphate–100 m*M* sodium tetraborate (pH 8); identification of peaks and other conditions are the same as in Fig. 3.

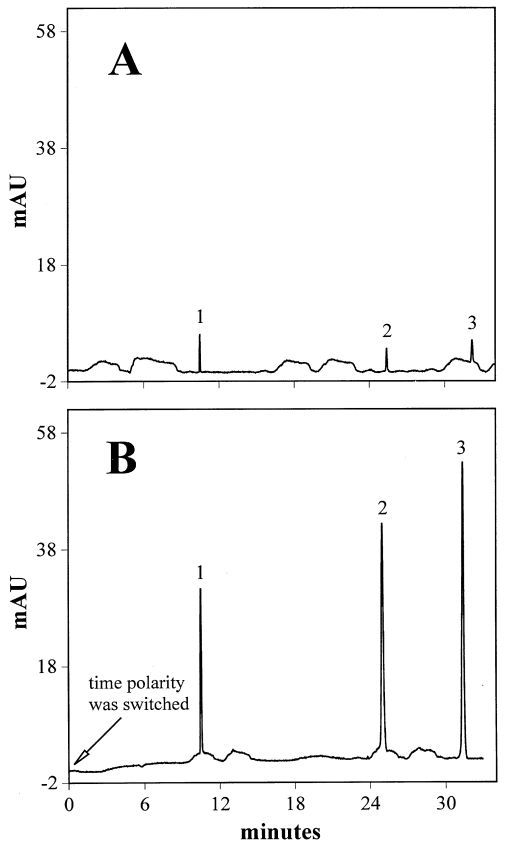

Fig. 5. Optimized REPSM electropherogram of test analytes with SDS; injection, 2 s (A), 90 s with matrix removal (B); S, samples in water; BGS; 130 m*M* SDS in 12.5 m*M* sodium dihydrogen phosphate–100 m*M* sodium hydroxide (pH 7); peaks: 1 (resorcinol), 2 (1,6-dihydroxynaphthalene), 3 (1-naphthol); capillary, 64.5 cm (56 cm to detector); detection, 214 nm.

4.2. Effect of analyte k on peak heights and peak areas

Figs. 4 and 5 show that stacking is very dependent on analyte *k*. In the analysis of naphthols using BBMA (Table 1), SE_{height}, SE_{area}, %SE and %*R* all increased with the increase in *k* as expected from the theory. A similar trend was observed in a BGS with SDS using resorcinol, 1,6-dihydroxynapthalene and 1-naphthol as test analytes (Table 2). In addition, based on the values of SE_{height}, an order of magnitude improvement in concentration detection limit can therefore be expected for the naphthols (Table 1) and the naphthalene derivatives (Table 2). Values for %Stacked are almost the same in the system with BBMA and are fairly close in the system with SDS. The effect of the nature of pseudostationary phases on peak heights and peak areas will be discussed in a later section.

4.3. Evidence of stacking by switching polarity at different percentages of current

By switching polarity at varying values of current at negative polarity (90, 95 and 99%) and looking at %*R*, we determined whether the neutral analyte is being carried to the concentration boundary by the fast moving micelle. Basically in non-stacking mode, peak areas increase with the increase in injected volume. For a solute that is not stacked (e.g. those with low *k* values), reducing the percentage of current when the polarities are switched will just increase the volume of injected sample compared to the volume injected when polarity is switched later (e.g., 99% current). Thus, an increase in %*R* should be observed with decreasing percentage of current when polarities are switched. In stacking mode, we assumed that the majority of the analytes as a consequence of stacking should have been brought near or within the concentration boundary at the instances when currents are between 90% and 99%. Therefore, %*R* should not dramatically increase specially for higher *k* analytes. The %*R* for the three test analytes at varying values of current when polarities are switched are given in Table 3 using SDS as pseudostationary phase. As expected for

Table 1
Effect of *k* on peak heights and peak areas with BBMA

Sample	SE_{height}	SE_{area}	%SE	%*R*	%Stacked
2-Naphthol	27.9	56.6	23.3	47.2	49.3
1-Naphthol	44.7	101.4	37.3	84.5	44.1

Note: conditions are the same as in Fig. 4.

Table 2
Effect of k on peak heights and peak areas with SDS

Sample	SE_{height}	SE_{area}	%SE	%R	%Stacked
Resorcinol	4.7	9.5	15.7	31.7	49.5
1,6-DHN	9.4	16.0	31.3	53.3	58.8
1-Naphthol	13.0	19.0	43.3	63.3	68.4

Note: conditions are the same as in Fig. 5.
1,6-DHN = 1,6-dihydroxynaphthalene.

Table 3
Effect of the time polarity was switched (%current) to %R

%Current	k	99%	95%	90%
Resorcinol	0.06	2%	13%	26%
1,6-DHN	1.46	29%	45%	51%
1-Naphthol	4.69	79%	85%	90%

S, samples in 5 mM sodium dihydrogen phosphate–10 mM sodium tetraborate (pH 7); BGS, 15 mM SDS in 50 mM sodium dihydrogen phosphate–100 mM sodium tetraborate (pH 7); injection, 90 s with matrix removal; capillary, 64.5 cm (56 cm to the detector); detection, 214 nm.

resorcinol (lowest k), %R increased with the decrease in the current when polarities are switched. For the other two test analytes, %R did not increase significantly with decrease in current especially with the highest retention factor analyte (1-naphthol). This also provides information about the dependence of analyte retention factors to stacking.

4.4. Experimental verification of x^*_{max}

In Table 4, we list x^*_{max} values (theoretical or computed and observed). Here we used the cmc of SDS (8 mM) as the concentration of surfactant in the S region and assumed that k is directly related to the concentration of surfactant. Getting the true value of x^*_{max} is not very critical as we are only interested in confirming the relationship between k_S and x^*_{max}. The x^*_{max}(observed) is based on the injection time wherein there are no significant increase in peak heights between consecutive injection intervals (see Fig. 6). Although the experimentally determined values for 1,6-dihydroxynapthalene and 1-naphthol are at least three orders lower compared to the theoretically determined ones, trends of theoretically and experimentally determined values are in agreement as predicted. Generally, x^*_{max} increased with the increase in k_S. The lower experimental values can be explained by the instability of the SDS micelle, causing ineffective stacking of neutral analytes. The effects of the nature of the pseudostationary phase will be discussed below.

Table 4
Computed and experimentally determined values of x^*_{max}

Sample	k	k_S	x^*_{max}	
			Computed	Observed
Resorcinol	0.06	0.03	0.02	~0.03
1,6-DHN	1.46	0.79	0.28	>0.07
1-Naphthol	4.69	2.53	0.46	~0.14

Note: conditions are the same as in Table 3.

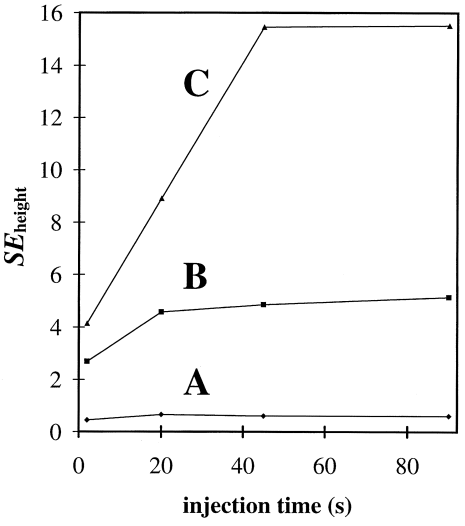

Fig. 6. Effect of the fraction of capillary filled with S on the stacking enhancement factors of neutral analytes. (A) Resorcinol; (B) 1,6-dihydroxynaphthalene; (C) 1-naphthol; conditions are the same as in Table 3.

4.5. Improving SE_{height} by increasing retention factors

SE_{height} increased with the increase in concentration of SDS (see Fig. 7). This is due to the increase in k_S as discussed in Section 2.4 and also due to the increase in the field enhancement factor γ. Run currents rose from 15 mA to 51 mA as the concentration of SDS is increased from 20 to 130 m*M*, implying that the conductivity of the BGS increased significantly due to the increase in the concentration of SDS. With SDS, we found that the concentration of the run buffer should be kept low while the concentration of SDS brought to a maximum value to achieve higher stacking enhancement factors without compromise to migration times. Higher concentrations of run buffer and SDS resulted in very long migration times (more than 90 min with an effective capillary length of 56 cm) due to reduction of electroosmotic flow velocity and very high retention factors. Peak broadening or splitting of higher retention factor compounds is also observed. With BBMA since solubilization of neutral analytes is less compared to SDS, running at relatively high concentrations of both surfactant and run buffer did not result in very long migration times.

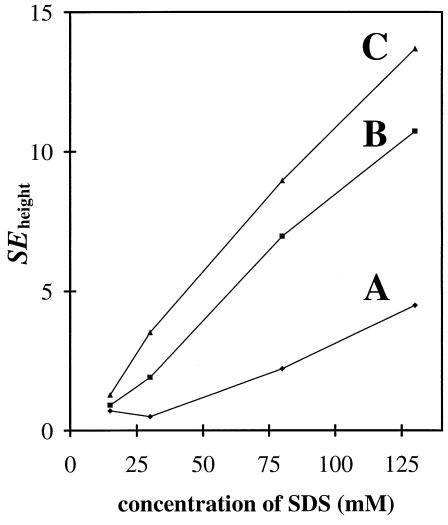

Fig. 7. Effect of the concentration of surfactant on the stacking enhancement factors of neutral analytes. (A) Resorcinol; (B) 1,6-dihydroxynaphthalene; (C) 1-naphthol; conditions are the same as in Fig. 5.

Addition of a non-ionic surfactant to the BGS increased peak heights compared to a BGS without the utilized non-ionic surfactant as mentioned in Section 2.4. This is depicted in Fig. 8. Improvement of detector response is higher with high retention factor compounds 1,6-dihydroxynaphthalene and 2-naphthol. Addition of non-ionic surfactant is therefore useful in improving stacking enhancement factors aside from providing added selectivity to a separation process.

4.6. Effect of the nature of the pseudostationary phases on peak heights and peak areas

Listed in Table 5 are the SE_{height}, SE_{area}, %SE, %*R* and %Stacked of resorcinol using the surfactants employed in this study. Values are significantly higher with high molecular mass surfactants HMMS (SUA and BBMA) compared to a low molecular mass surfactant LMMS (SDS). The electropherograms for each surfactant are shown in Fig. 9, sharper peaks are obtained with HMMS (C,D). This could be explained by the stable molecular micelle nature of HMMS (zero cmc). In the case of LMMS, the

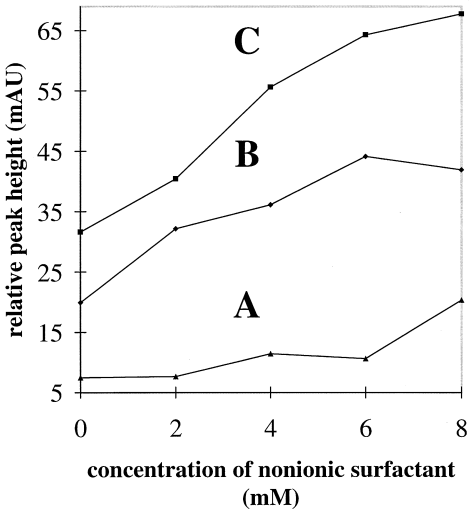

Fig. 8. Effect of the addition of non-ionic surfactant (Brij 35) on the improvement of detector responses of neutral analytes. (A) Resorcinol; (B) 1,6-dihydroxynaphthalene; (C) 2-naphthol; BGS, 1% BBMA and 0, 2, 4, 6, 8 m*M* Brij 35 in 50 m*M* sodium dihydrogen phosphate–100 m*M* sodium tetraborate (pH 8); injection, whole capillary filling REPSM; S, samples in water; capillary, 63.5 cm (55 cm to the detector); detection, 210 nm.

Table 5
Effect of the nature of the surfactants to peak heights and peak areas of resorcinol

	100 m*M* SDS	1% SUA	1% BBMA
SE_{height}	9.2	35.6	42.6
SE_{area}	7.4	23.8	19.0
%SE	7.7	29.7	35.5
%*R*	6.2	19.8	15.8
%Stacked	104.1	124.8	187.2

Note: conditions are the same as in Fig. 9.

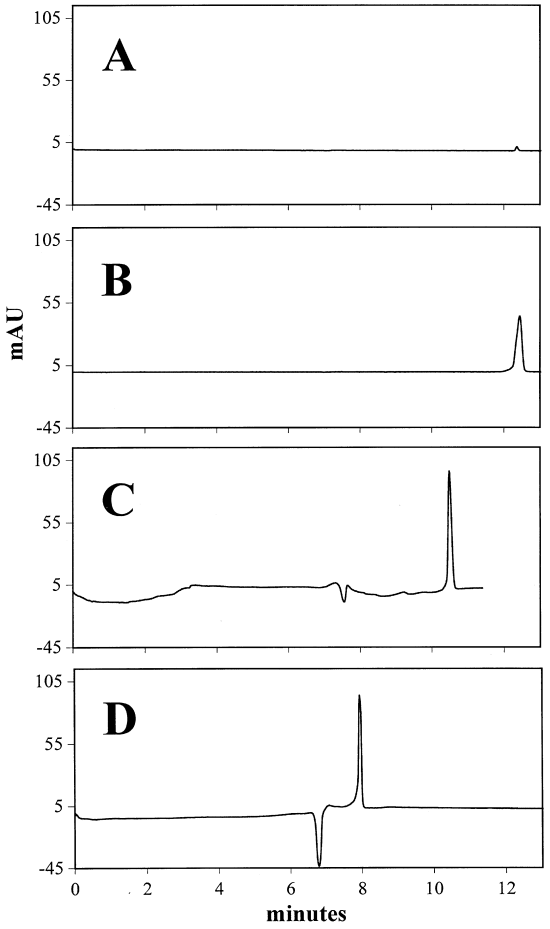

Fig. 9. Comparison of stacking effects among different surfactants. BGS, 100 m*M* SDS in run buffer (A,B), 1% SUA oligomer in run buffer (C), 1% BBMA in run buffer (D); injection, 2 s (A), whole capillary filling REPSM (B,C,D); S, resorcinol in water; run buffer, 50 m*M* sodium dihydrogen phosphate–100 m*M* sodium tetraborate (pH 8); capillary, 63.5 cm (55 cm to the detector); detection, 210 nm.

concentration of surfactant micelles was probably too low in the S region due to dilution to cause efficient stacking. The calculated values for %*R* are rather low while values for %SE are rather high causing %Stacked values greater than 100% for all surfactants studied. This can be explained by the high value of γ in all these systems. Calibration curves within a concentration range of $1.135 \cdot 10^{-4}$ *M* and $4.540 \cdot 10^{-6}$ *M* are constructed for the systems in Fig. 9. Linear regression analysis equations are as follows: $y = 0.9170x + 1.1310$, $r = 0.9999$ and CL = 4.22×10^{-6} *M* (100 m*M* SDS with 2 s injection); $y = 1.2873x + 3.7177$, $r = 0.9994$ and CL = 1.06×10^{-6} *M* (100 m*M* SDS with REPSM); $y = 0.8125x + 2.2162$, $r = 0.9918$ and CL = $1.06 \cdot 10^{-7}$ *M* (1% SUA oligomer with REPSM); $y = 0.8153x + 2.3297$, $r = 0.9393$ and CL = $1.05 \cdot 10^{-7}$ *M* (1% BBMA with REPSM); *y* is the logarithm of the peak height (AU), *x* is the logarithm of the molar concentration of resorcinol and CL is the concentration detection limit ($S/N = 3$).

In conclusion, REPSM is shown to be a very promising method, with enhanced detection sensitivity of neutral analytes in MEKC. Over an order of magnitude improvement in concentration detection limit has been demonstrated using HMMS. Compared with the normal stacking mode, an advantage is that it affords a much larger injection volume of sample solutions into the capillary and thus higher stacking enhancement factors. Careful selection of analytical parameters (i.e., concentration of surfactant and buffer components in BGS) will permit the stacking and separation of both low and moderately high retention factor compounds and will yield reasonable migration times. Application of this technique to complex samples (samples containing a great number of analytes) and real samples (analytes in real matrices like lake or river water) is the objective of future studies. A sample clean-up step will be necessary for the analysis of real samples.

5. List of symbols

a	A neutral analyte
B_1	Concentration boundary
B_2	Boundary separating the re-

	gion of micelles coming from the cathodic vial from the rest of the S region during step 2
BGS	High conductivity background solution
E_0	A voltage (V) applied across a capillary with length (L)
E_S	Enhanced local field strength in the S region
E_{BGS}	Local field strength in the BGS region
γ	Enhancement factor
H	Height obtained with non-stacking MEKC
H_{stack}	Height obtained with REPSM MEKC using the same solution used for obtaining H
k	Retention factor of a neutral analyte
k_S	Retention factor of a neutral analyte in the S region
k_{BGS}	Retention factor of a neutral analyte in the BGS region
L	Length of the capillary
μ_{eof}(S)	Coefficient of electroosmotic flow of S
μ_{ep}(mc)	Electrophoretic mobility of the micelle
%R	Percentage recovery in terms of peak areas
S	Low conductivity sample solution
%SE	Percentage of sample effectively stacked into a peak from the total volume of sample injected
%Stacked	Amount of analyte that is effectively stacked from the total amount of analyte that resisted the electroosmotic flow after step 2
SE_{height}	Experimentally determined stacking enhancement factor in terms of peak height
SE_{height} (expected)	Expected stacking enhancement factor in terms of peak height
SE_{area} (observed)	Experimentally determined stacking enhancement factor in terms of corrected peak areas
SE_{area} (expected)	Expected stacking enhancement factor in terms of peak area
V	Constant voltage applied
v_a(BGS)	Migration velocity of a in the BGS region during step 2
v_a(S)	Migration velocity of a in the S region during step 2
v_{ep}(mc,BGS)	Electrophoretic velocity of the micelle in the BGS region
v_{ep}(mc,S)	Electrophoretic velocity of the micelle in the S region
v_{eof}(BGS)	Electroosmotic velocity of BGS
v_{eof}(S)	Electroosmotic velocity of S
v_{eof}(ave)	Averaged electroosmotic velocity of the entire solution inside the capillary
v^*_{ep}(a,BGS)	Effective electrophoretic velocity of a in the BGS region
v^*_{ep}(a,S)	Effective electrophoretic velocity of a in the S region
v_{mc}(BGS)	Migration velocity of the micelle in the BGS region
v_{mc}(S)	Migration velocity of the micelle in the S region
x	Fraction of the capillary filled with S
x_{max}	Ultimate maximum fill fraction
x^*_{max}	Maximum fill fraction for a neutral analyte

Acknowledgements

The authors are thankful to Dr. Otsuka, Dr. Matsubara, Dr. Muijselaar and Mr. Iida for their support. JQ is also grateful to the Ministry of Education, Science, Culture and Sports, Japan for the scholarship and the University of the Philippines Manila for allowing him to go on leave. This work was supported in part by a Grant-in-Aid for Sci-

entific Research (No. 07554040) from the Ministry of Education, Science, Culture, and Sports, Japan.

References

[1] S. Terabe, K. Otsuka, K. Ichihara, A. Tsuchiya, T. Ando, Anal. Chem. 56 (1984) 111–113.
[2] Z. Liu, P. Sam, S.R. Sirimanne, P.C. McClure, J. Grainger, D.G. Patterson, J. Chromatogr. A 673 (1994) 125–132.
[3] J.P. Quirino, S. Terabe, J. Chromatogr. A 781 (1997) 119–128.
[4] K.R. Nielsen, J.P. Foley, J. Chromatogr. A 686 (1994) 283–291.
[5] R.L. Chien, D.S. Burgi, Anal. Chem. 64(8) (1992) 489A–496A.
[6] D.S. Burgi, R.L. Chien, J. Microcol. Sep. 3 (1991) 199–202.
[7] D.S. Burgi, R.L. Chien, Anal. Chem. 63 (1991) 2042–2047.
[8] R.L. Chien, D.S. Burgi, J. Chromatogr. 559 (1991) 141–152.
[9] R.L. Chien, D.S. Burgi, J. Chromatogr. 559 (1991) 153–161.
[10] R.L. Chien, D.S. Burgi, Anal. Chem. 64 (1992) 1046–1050.
[11] D.S. Burgi, Anal. Chem. 65 (1993) 3726–3729.
[12] R.L. Chien, J.C. Helmer, Anal. Chem. 63 (1991) 1354–1361.
[13] S. Terabe, J. Pharm. Biomed. Anal. 10 (1992) 705–715.
[14] C.P. Palmer, M.Y. Khaledi, H.M. McNair, J. High Resolut. Chromatogr. 15 (1992) 756–762.